

Crack growth under static and fatigue loading in glassy polymers oriented by cold-rolling

M. Kitagawa, S. Isoke and H. Asano

Department of Mechanical Engineering, Faculty of Technology, Kanazawa University, Kanazawa, Japan

(Received 16 November 1981; revised 8 March 1982)

Static and fatigue crack growth in PC and fatigue crack growth in PVC have been studied using anisotropic sheets oriented by cold-rolling. Tests were carried out at room temperature for samples with various degrees of rolling reduction. In static loading for PC, a slight rolling reduction considerably improves the resistance to crack propagation in the case where the crack grows perpendicularly to the rolling direction. The measured values of crack opening displacement were compared with the Dugdale model, taking into account the effect of anisotropy. In fatigue loading for both polymers used, a power law relationship between crack growth rate dc/dN and stress intensity factor range ΔK , i.e., $dc/dN = A(\Delta K)^m$ where A and m are constants, covers most of the data in spite of the differences in degrees of anisotropy. However, the constants A and m are dependent on the degree of rolling reduction. In PVC, the rolling reduction changes the fatigue fracture mode from a discontinuous growth type to continuous one. All the results show that the rolling reduction has an important effect on crack behaviour.

Keywords Crack growth; cold-rolling; anisotropy; striation; glassy polymer; opening displacement

INTRODUCTION

Much effort has been put in to understanding the mechanism of crack growth in polymer solids. A large proportion of the experimental results demonstrate that the rates of static and fatigue crack growth are well described by fracture mechanics parameters such as stress intensity factor and strain energy release rate^{1,2}. Materials used for these studies were generally recognized as isotropic. But practically speaking most polymers used are more or less anisotropic due to anisotropic formation processes. However, little attention has been paid to the experimental problems of a crack embedded in an anisotropic body, whereas there has been much data published on the yielding of samples oriented by hot drawing³. This is probably due to the difficulty that test pieces, which are wide and uniform enough to observe the behaviour of crack, are not easily prepared. Cold-rolling is used here and this process is able to make wide uniform plates with arbitrary degrees of anisotropy. Although a series of studies was made on the improvement of the mechanical properties of cold-rolled samples such as yield stress, impact strength and crazing stress by Broutman^{4,5} and one of these authors (Kitagawa)^{6,7}, crack problems have remained unresolved. However, fibre reinforced plastics (FRP) may be used in gaining an understanding of crack behaviour⁸. But the crack difficulties associated with FRP seem to be more complex than that of a simple polymer solid because of the mutual interaction between the fibre and its matrix.

The purpose of this paper is, therefore, to take a first step in investigating the crack problems of anisotropic polymers and to provide some experimental data about them.

EXPERIMENTAL

Materials used were polycarbonate (PC) and poly(vinyl chloride) (PVC) plates 2 mm thick (Takiron Co., Japan). Rectangular sheets (75 × 200 mm) were cut from these plates and uniaxially cold-rolled at room temperature with a home-made rolling mill, the details of which were reported elsewhere⁶. The reduction in thickness through rolling was less than 0.1 mm with every pass. The sheets were progressively rolled to the desired ratios of rolling reduction r , r being defined as $h_0 - h/h_0 \times 100\%$ where h_0 and h were the initial final thicknesses of the sheet. The reduction ratios were chosen in the range up to 60%, since cracking resulted during rolling in excess of $r = 60\%$. After rolling, the rolled plates of PC were annealed for 1 hour at 120°C and slowly cooled to room temperature in an electric oven. During annealing, the rolled sheets were placed between glass plates tightly bound between steel plates, to prevent the sheets returning to their original shape as before rolling. The as-received ($r = 0\%$) plates of PC were annealed for 1 hour at the glass transition temperature (155°C) and alternatively the PVC samples were prepared without annealing.

Dumb-bell shaped specimens (30 mm long and 10 mm wide in gauge section) were cut from the rolled plates so that their axes were inclined at various orientation angles, θ , to the rolling direction as shown in *Figure 1*, and were pulled at a strain rate of 7×10^{-3} /min at room temperature with an Instron type tensile testing machine.

Single edge notched (SEN) specimens with various values of θ were prepared for both static and fatigue tests. The initial notches 5 to 10 mm long were introduced by a fillet saw and a razor blade. All fatigue tests were conducted with zero-tension loading at room

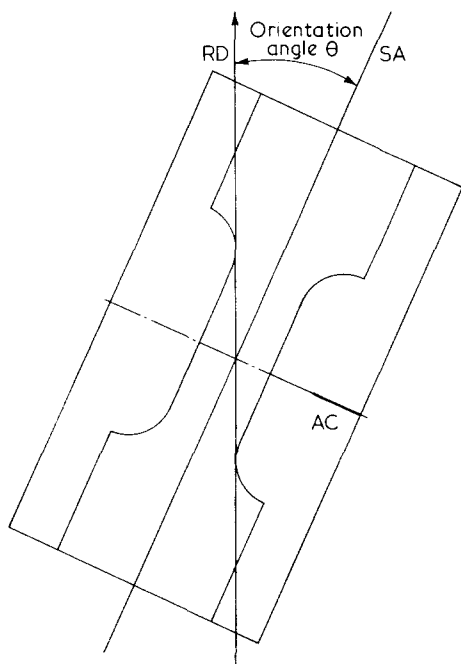


Figure 1 Schematic illustration of specimen orientation. RD: rolling direction; SA: specimen axis; AC: artificial crack perpendicular to SA

Table 1 Experimental values of yield stress σ_Y and elastic modulus E for various reduction ratios r and orientation angles θ in PC

| r (%) | $\theta = 0^\circ$ | 30° | 45° | 60° | 90° | |
|---------|--------------------|------------|------------|------------|------------|------|
| 0 | σ_Y | 74.3 | | | | |
| | E | 2330 | | | | |
| 20 | σ_Y | 71.3 | — | — | 62.5 | |
| | E | 2770 | | | 2620 | |
| 30 | σ_Y | 80.9 | 75.6 | 71.1 | 66.6 | 64.3 |
| | E | 2910 | 2890 | 2760 | 2680 | 2650 |
| 40 | σ_Y | 89.9 | — | — | — | 63.8 |
| | E | 3030 | | | | 2590 |
| 50 | σ_Y | 104.0 | 86.4 | 76.6 | 67.4 | 62.8 |
| | E | 3430 | 3150 | 2820 | 2730 | 2690 |

* Units of σ_Y and E in MPa

temperature ($20^\circ \pm 1^\circ\text{C}$). The test frequency was in the range 0.25 to 0.4 Hz. During each fatigue test, the maximum load was controlled and was held constant. Crack growth rates were measured with the aid of a travelling microscope. The stress intensity factor range for this specimen configuration is⁹

$$\Delta K = Y\Delta\sigma\sqrt{c} \quad (1)$$

where $Y = 1.99 - 0.041(c/w) + 18.70(c/w)^2 - 38.48(c/w)^3 + 53.85(c/w)^4$, c is the crack length, W is the specimen width and $\Delta\sigma$ is the applied stress range. Although equation (1) may not always be valid for an anisotropic specimen with finite width, it is used for simplicity here.

RESULTS AND DISCUSSION

Static tension

Experimental values of elastic modulus E and peak yield stress σ_Y of PC are listed in Table 1. It is found that

both values of E and σ_Y along the rolling direction ($\theta = 0^\circ$) increase with an increase in r and decrease with increasing θ for constant r . These trends are similar to previous results⁶.

Figure 2 shows the variation of apparent fracture toughness K_a with r . The apparent fracture toughness, which is defined as the value at which the initial crack begins to grow, is calculated from equation (1). K_a increases with increasing r for a $\theta = 0^\circ$ specimen, but decreases for a $\theta = 90^\circ$ specimen. Figure 3 describes the variations of K_a and crack growth direction Ψ with θ . The direction of crack growth is not always perpendicular to the loading axis, as shown in Figure 3. For $\theta = 90^\circ$, the plastic zone grown approximately along the initial crack axis. This trend becomes evident in excess of $r = 50\%$. It is surprising that even the crack placed in the direction of

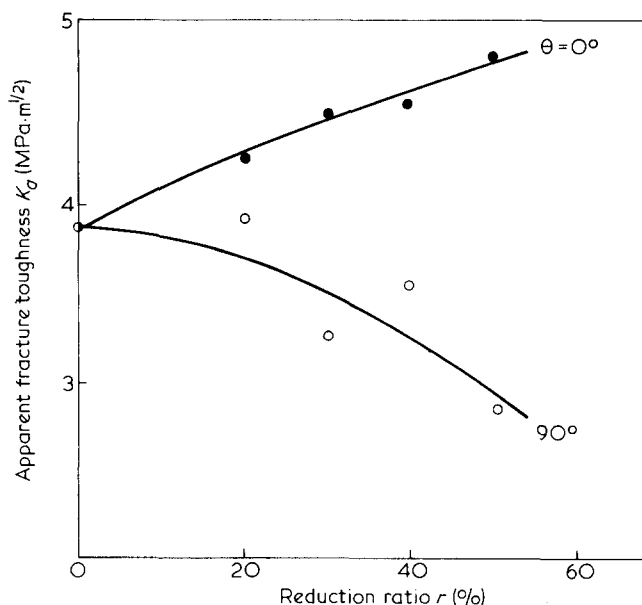


Figure 2 Effect of reduction ratio on apparent fracture toughness in PC

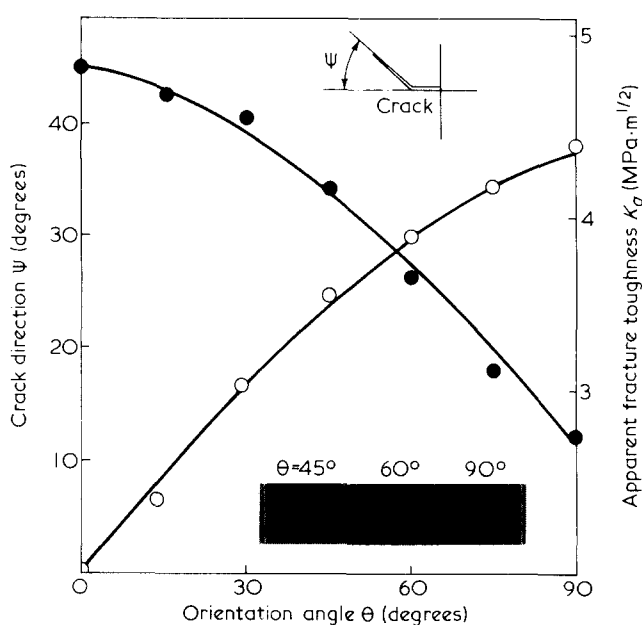


Figure 3 Orientation dependence of crack growth direction and apparent fracture toughness in PC (reduction ratio: 50%)

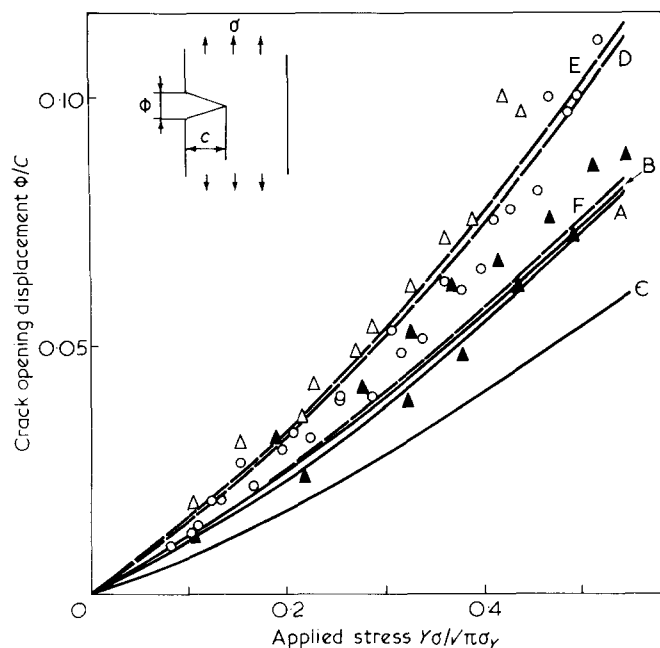


Figure 4 Relationship between crack opening displacement and applied stress for PC samples with reduction ratios 0% (○) and 50% (△, ▲). The open and solid triangles denote the data points of $\theta = 0^\circ$ and 90° , respectively. The solid curves represent equation (4) for $r = 0\%$ (A), $r = 50\%$ and $\theta = 0^\circ$ (B) and $\theta = 90^\circ$ (C). The broken curves indicate the modified equation for $r = 0\%$ (D), $r = 50\%$ and $\theta = 0^\circ$ (E) and $r = 50\%$ and $\theta = 90^\circ$ (F)

the rolling becomes curved despite the weakness along the crack axis.

Experimental relations between crack opening displacement ϕ and applied stress σ are shown for $r = 0$ and 50% in Figure 4, where the applied stress is normalized by the tensile yield stress σ_Y in each direction. The opening displacement used here is defined in Figure 4. To avoid the effect of specimen geometry on the stress intensity factor, the applied stress is replaced by a corrected stress ($Y/\sqrt{\pi}$) σ so that the stress intensity factor for a SEN specimen, $Y\sigma\sqrt{c}$, may become equivalent to that for an infinite plate, $\sigma\sqrt{\pi c}$. The values of ϕ arranged in this way are slightly higher for a $\theta = 0^\circ$ specimen than for a $\theta = 90^\circ$ specimen. This trend is also observed in the case where $r = 30\%$.

According to the orthotropic Dugdale model, the length of plastic zone ahead of the crack, s , and the opening displacement, v , at a distance x along the crack axis from the crack centre, are given by

$$\frac{c}{c+s} = \cos\left(\frac{\pi}{2} \frac{\sigma}{\sigma_Y}\right) \quad (2)$$

and

$$v = \eta \frac{\sigma_Y(c+s)}{\pi E_2} \left\{ \cos \xi \ln \left[\frac{\sin^2(\beta - \xi)}{\sin^2(\beta + \xi)} \right] + \cos \beta \ln \left[\frac{(\sin \beta + \sin \xi)^2}{(\sin \beta - \sin \xi)^2} \right] \right\} \quad (3)$$

respectively, where $\eta = \sqrt{2E_2/E_1} [\sqrt{E_1/E_2 + (E_1/2G_{12}) - \nu_1}]^{1/2}$, $\beta = (\pi/2)(\sigma/\sigma_Y)$, $\xi = \cos^{-1}[x/(c+s)]$, σ_Y is the yield stress along the tensile direction, ν is Poisson's ratio, E the elastic modulus, G the shear modulus and the indices 1 and 2 denote the principal axes of anisotropy. Equation (3) is obtained on the assumption that the tensile axis is parallel to direction 2. When $\xi = \pi/2$, equation (3) reduces to

$$\phi(=2v_{x=0}) = 2\eta \frac{c \sigma_Y}{\pi E_2} \ln \left(\frac{1 + \sin \beta}{1 - \sin \beta} \right)^2 \quad (4)$$

For an isotropic body η is set as equal to 2. The elastic factor η can be calculated from the data in Table 1 and the equation

$$4/E_{45} = 1/E_1 + 1/E_2 + (1/G_{12} - 2\nu_1/E_1) \quad (5)$$

where E_{45} is the elastic modulus in the direction inclined at 45° to the tensile axis. The values of η calculated in this way are approximately 2.03 for $r = 30\%$, $\theta = 0^\circ$; 1.98 for $r = 30\%$, $\theta = 90^\circ$; 2.14 for $r = 50\%$, $\theta = 0^\circ$ and 2.00 for $r = 50\%$, $\theta = 90^\circ$. All the values are nearly equal to the isotropic value. The solid curves in Figure 4 denote equation (4) for $r = 0$ and 50%, with σ_Y/E_2 being given in Table 1. The solid theoretical curves are slightly lower than the measured values. The discrepancy between the solid theoretical curves and the measured values may be attributed to experimental error and the data arrangement by use of the corrected stress adopted here. Equation (4) was modified so that the theoretical curve (A) may fit the isotropic data, being multiplied by an empirical factor 1.4. The modified equation for the isotropic case ($\eta = 2$) is given by the broken curve (D). The broken curves (E) and (F) show the result of $r = 50\%$ for $\theta = 0^\circ$ and 90° , respectively, calculated by use of the modified equation with a proportional factor 1.4. The broken curves show that the data for $\theta = 0^\circ$ are higher than the data for $\theta = 90^\circ$. This arises mainly from the fact that the ratio σ_Y/E_2 is higher in the $\theta = 0^\circ$ direction than in the $\theta = 90^\circ$. The relative positions of each curve are therefore governed by the factor σ_Y/E_2 rather than the elastic factor η .

The plastic zone was not at all distinct except for specimens taken from the $r = 0\%$ and 30% sheets. The results obtained from both samples showed that equation (2) was in good agreement with the experimental data.

The above results indicate that a slight rolling reduction improves the static strength K_u of PC in the direction parallel to the rolling. Furthermore, it is clear that the elastic factor η does not play an important role in the data arrangement for crack opening displacement in this anisotropy range.

Fatigue crack growth

Examples of the relationship between fatigue crack growth rate dc/dN and stress intensity factor range ΔK are shown for PC in Figure 5, where the solid curves are drawn by means of the least-square method. For PC samples with $r = 50\%$ and $\theta = 90^\circ$, the crack becomes curved and did not propagate along the direction perpendicular to the loading axis for fatigue as well as for static tension. However, in the other cases described below, the fatigue crack growth occurred approximately along the initial crack axis. Therefore, the data for $r = 50\%$

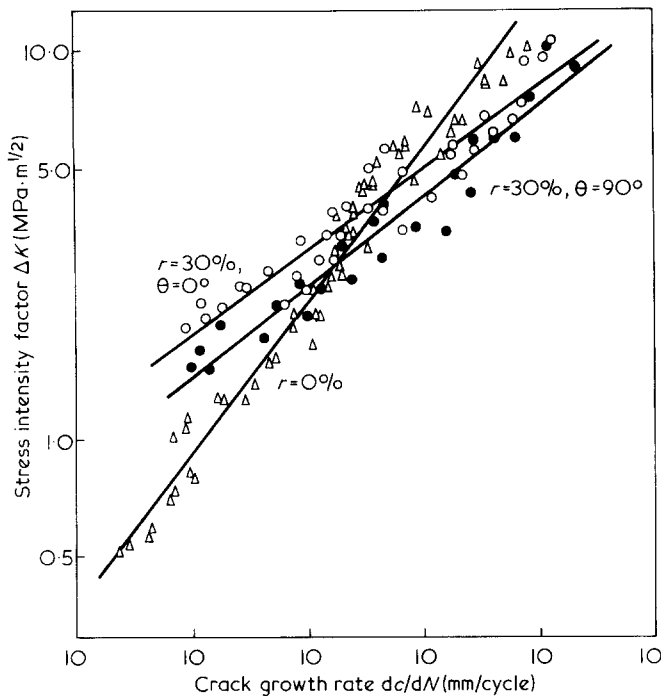


Figure 5 Examples of relationship between stress intensity factor range and crack growth rate in PC

and $\theta=90^\circ$ samples are omitted. It is found that a power law relationship between dc/dN and ΔK

$$\frac{dc}{dN} = A(\Delta K)^m \quad (6)$$

can be successfully applied to the data for PC.

The results are summarized for both polymers used, in Figure 6 and Figure 7. The solid and broken curves in Figure 7 represent the results for $\theta=0^\circ$ and 90° , respectively. The lines in Figure 6 are obtained by the least-square method, but in Figure 7 they are drawn empirically. At high ΔK levels in PVC, the power law equation appears to be valid.

It is clear that a slight reduction in thickness due to rolling, increases the resistance to fatigue crack growth especially at low ΔK levels in either of the $\theta=0^\circ$ and 90° directions. This seems to contradict the static result for Figure 2 where K_a decreases with increasing r in the case of $\theta=90^\circ$. This contradiction is probably due to the difference between the cyclic and static loadings.

The values for the constants A and m for PC, calculated by the least-square method, are given in Table 2. The exponent m tends to increase as the extent of anisotropy increases. In other words, the constants A and m in equation (1) depend on the degree of reduction in thickness.

Fatigue fracture surfaces were observed with an optical microscope. The fracture surfaces of the rolled samples of PC have a feature similar to those of unoriented materials namely so-called 'striations', which form during each load cycle, and their spacings become greater as ΔK increases. This feature seems to be independent of the extent of rolling reduction.

Typical fracture markings of PVC are shown in Figure 8. In unoriented PVC, another series of parallel markings, called discontinuous growth bands by Skibo *et al.*¹⁰, are

evident in the entire range of ΔK tested. Although these bands are also perpendicular to the direction of crack growth, like to the striations, each band is not formed during one load excursion. Skibo *et al.* suggested that the formation process of these bands is closely related to the local plastic or craze zone ahead of the crack tip. However, for rolled PVC samples, the striations but not the discontinuous growth bands, are observed at the levels of ΔK tested, no matter how the samples are inclined to the rolling direction. Even in a rolled plate, with only 10%

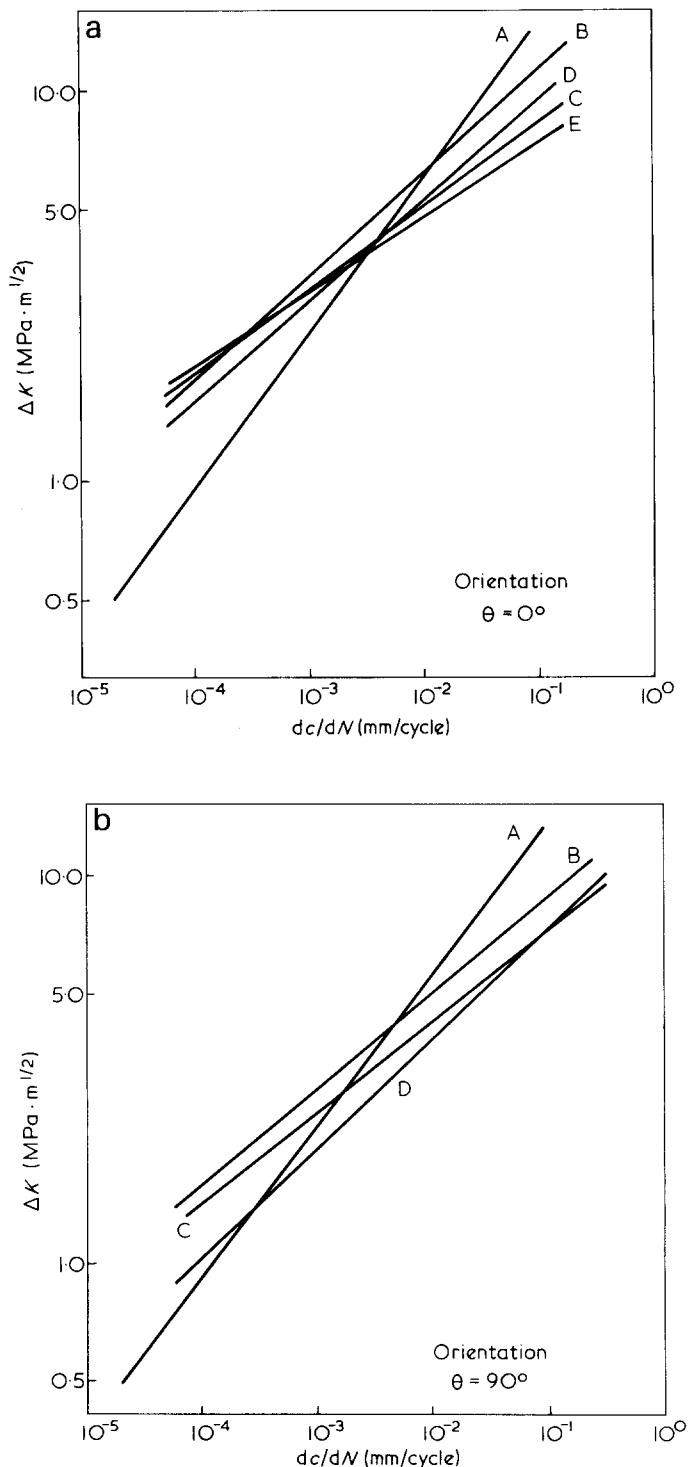


Figure 6 Summary of relationship between stress intensity factor and fatigue crack growth rate for various reduction ratios in PC. Curve (A), $r = 0\%$; (B), $r = 20\%$; (C), $r = 30\%$; (D), $r = 40\%$; (E), $r = 50\%$. (a) $\theta = 0^\circ$, (b) $\theta = 90^\circ$

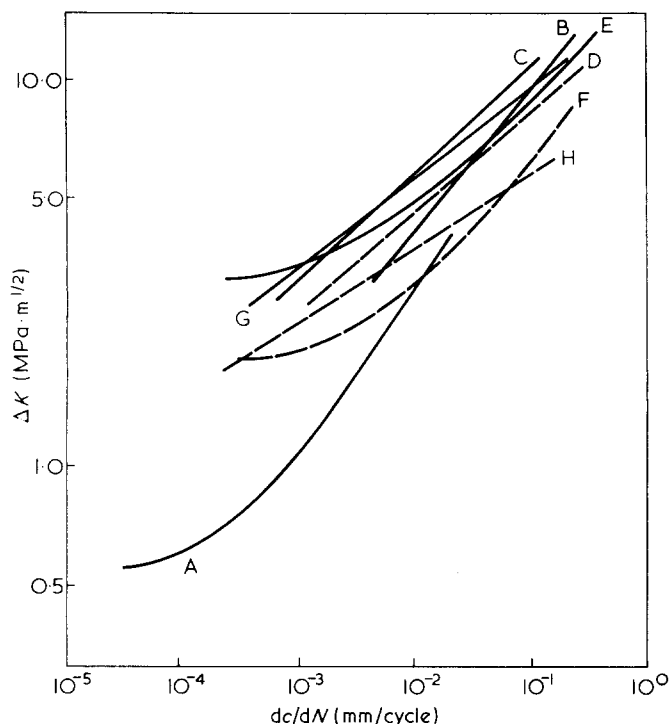


Figure 7 Summary of relationships between stress intensity factor and fatigue crack growth rate in PVC. The solid and broken curves denote the curves for $\theta = 0^\circ$ and 90° , respectively. Curve (A), $r = 0\%$; (B), $r = 10\%$; (C), (D), $r = 30\%$; (E), (F), $r = 50\%$; (G), (H), $r = 60\%$

Table 2 Values of the constants in equation (6) calculated from the least-square method in PC

| r (%) | θ ($^\circ$) | m | A |
|---------|-----------------------|------|-----------------------|
| 0 | | 2.52 | 1.17×10^{-4} |
| 20 | 0 | 3.85 | 1.03×10^{-5} |
| | 90 | 4.00 | 1.49×10^{-5} |
| 30 | 0 | 4.67 | 0.54×10^{-5} |
| | 90 | 4.20 | 1.37×10^{-5} |
| 40 | 0 | 3.97 | 1.59×10^{-5} |
| | 90 | 3.50 | 0.87×10^{-5} |
| 50 | 0 | 5.31 | 3.11×10^{-6} |
| | 45 | 3.58 | 4.08×10^{-5} |

* Units of dc/dN and ΔK in mm/cycle and $MPa \cdot m^{1/2}$ respectively

reduction, the discontinuous bands cannot be observed. The plastic deformation due to rolling seems to change the mode of fatigue crack growth from the discontinuous to the continuous type.

CONCLUSION

Static and fatigue crack growth in PC and fatigue crack growth in PVC were investigated using anisotropic sheets oriented by cold-rolling. The results are summarized as follows;

(1) A slight rolling reduction in thickness improves the resistance to static crack growth for PC and the resistance to fatigue crack growth at low values of ΔK for both PC and PVC especially along the rolling direction.

(2) The measured crack opening displacement is in good agreement with the orthotropic Dugdale model. In the extent of rolling reduction up to 60% for PC, the

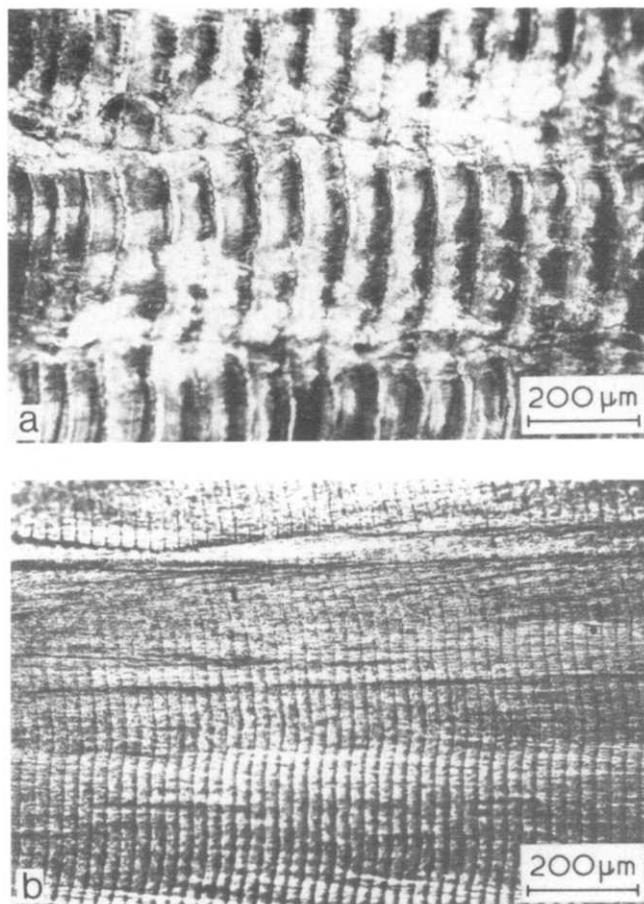


Figure 8 Fatigue fracture surfaces of PVC. (a) $r = 0\%$, discontinuous growth band. (b) $r = 30\%$, continuous growth band

elastic factor (see equation (3)) does not necessarily play an important role in the model, but the ratio of yield stress to elastic modulus along the tensile direction becomes important.

(3) A power law relationship between dc/dN and ΔK holds for PC over the entire range of ΔK that was investigated, but it does not hold for PVC at low values of ΔK . The constants involved in the equation are greatly affected by the degree of rolling reduction.

(4) For PVC, a rolling reduction changes the mode of fatigue crack from discontinuous growth band type to continuous striation type, whereas PC exhibits only continuous striations.

REFERENCES

- For example (static), Atkins, A. G., Lee, C. S. and Caddle, R. M. *J. Mater. Sci.* 1975, **10**, 1381
- For example (fatigue), Sauer, J. A. and Richardson, G. C. *Int. J. Fracture* 1980, **16**, 499
- Brown, N., Duckett, R. A. and Ward, I. M. *Phil. Mag.* 1968, **18**, 483
- Broutman, L. J. and Patil, R. S. *Polym. Eng. Sci.* 1971, **11-2**, 165
- Broutman, L. J. and Krishnakumar, S. M. *ibid.* 1974, **14-4**, 165
- Kitagawa, M., Nozima, Y. and Ogawa, H. *J. Jpn. Soc. Tech. Plasticity* 1977, **18**, 85; 1977, **18**, 204; 1977, **18**, 344
- Kitagawa, M. and Ogawa, H. *J. Soc. Mater. Sci. Jpn.* 1976, **25**, 974
- Tirosh, J. *J. Appl. Mech., Trans. ASME* 1973, **40**, 785
- Srawly, J. E. and Brown, W. F., Jr. *ASTM STP*, 381, *Am. Soc. Testing Mats.* 1965, 133
- Skibo, M. D., Herzberg, R. W., Manson, J. A. and Kim, S. L. *J. Mat. Sci.* 1977, **12**, 531